

**Prediction of pressure-induced red shift of $f^1 \rightarrow d(t_{2g})^1$ excitations
in $\text{Cs}_2\text{NaYCl}_6:\text{Ce}^{3+}$ and its connection with bond length
shortening.**

Fernando Ruipérez,^a Luis Seijo,^b and Zoila Barandiarán^b

^{a,b}*Departamento de Química, C-XIV,*

Universidad Autónoma de Madrid, 28049 Madrid, Spain.

^b*Instituto Universitario de Ciencia de Materiales Nicolás Cabrera,*

Universidad Autónoma de Madrid, 28049 Madrid, Spain

(Dated: September 13, 2018)

Abstract

Quantum chemical calculations including embedding, scalar relativistic, and dynamic electron correlation effects on $\text{Cs}_2\text{NaYCl}_6:(\text{CeCl}_6)^{3-}$ embedded clusters predict (*i*) red shifts of the $f^1 \rightarrow d(t_{2g})^1$ transition with pressure and (*ii*) bond length shortening upon $f \rightarrow d(t_{2g})$ excitation. Both effects are found to be connected which suggests that new high pressure spectroscopic experiments could reveal the sign of the bond length change.

I. INTRODUCTION

Recent *ab initio* theoretical studies of the structure and spectroscopy of octahedral complexes of lanthanide/actinide ions have shown that the bond length between the *f*-element and the surrounding ligands shortens upon $f^n \rightarrow f^{n-1}d(t_{2g})^1$ excitation.^{1,2,3,4,5} This is so for different halide ligands (F, Cl, Br), environments (crystals, liquid solutions, gas phase), oxidation states of the f^n ion (III, IV), and number of *f* electrons (across the lanthanide/actinide series).^{1,2,3,4,5,6} Yet, it contradicts the widespread assumption that $f^n \rightarrow f^{n-1}d^1$ excitations lengthen the impurity-ligand bonds.^{7,8,9,10}

Usually, the materials involving *f*-element ion complexes are liquid or solid solutions and a direct experimental proof of the bond shortening could be obtained, in principle, by means of ground (f^n) and excited state ($f^{n-1}d^1$) EXAFS measurements. In this respect, a theoretical study of $(CeX_6)^{3-}$ (X= F, Cl, Br) complexes in cubic elpasolites, liquid acetonitrile solution, and gas phase, has pointed out the chloride and bromide complexes in acetonitrile as good candidates for excited state EXAFS experiments because the negative bond length shifts are largest and the liquid medium could favor the experimental setting.⁵ However, excited state EXAFS measurements are extremely demanding because the difficulties inherent to EXAFS experiments and their interpretation are extended by the need of pumping the samples onto the excited $f^{n-1}d^1$ levels for long periods of time and by the uncertainties on the actual excited state population attained. As a matter of fact, no successful experiments of this kind have yet been reported in octahedral complexes of *f* element ions in solid or liquid media, to our knowledge.

In this paper, on the basis of quantum chemical simulations, we propose that spectroscopic studies under high hydrostatic pressure^{11,12} are an alternative, relatively simple experimental technique to proof or reject the predicted bond length shortening upon $f^n \rightarrow f^{n-1}d(t_{2g})^1$ excitation. In effect, quantum chemical calculations in $Cs_2NaYCl_6:Ce^{3+}$ reveal that the shortening in bond length upon $f^n \rightarrow f^{n-1}d(t_{2g})^1$ excitation results in a continuous redshift of the transition energy with pressure in the range 1 bar – 26 kbar. More generally, the sign of the bond length change upon excitation determines the sign of the slope of the transition energy with pressure. As a consequence, the theoretically found sequence of bond lengths in octahedral complexes,⁴ $R_e[f^{n-1}d(t_{2g})^1] \leq R_e[f^n] \leq R_e[f^{n-1}d(e_g)^1]$, consistently leads to decreasing $f^n \rightarrow f^{n-1}d(t_{2g})^1$, constant $f^n \rightarrow f^n$, and increasing $f^n \rightarrow f^{n-1}d(e_g)^1$

transition energies with hydrostatic pressure. These results also enhance the value of high pressure experiments to alter the relative positions of excited states^{8,11,13} and to help the usually difficult assignment of the $f^{n-1}d(e_g)^1$ highest energy levels.¹⁴

II. RESULTS AND DISCUSSION

The effects of hydrostatic pressure on the local structure and electronic transitions of the $(\text{CeCl}_6)^{3-}$ defects in $\text{Cs}_2\text{NaYCl}_6$ were studied using the relativistic *ab initio* model potential (AIMP) embedded cluster method.^{15,16} More detailed descriptions of the method, as applied to *f* element ions in ionic crystals, can be found in Refs. 2 and 4. The effective core potentials used for Ce¹⁷ and Cl¹⁸ in an experimental and theoretical study of the absorption and emission spectra of Ce³⁺ in elpasolite lattices¹⁴ were also used here to incorporate scalar relativistic effects. In order to include dynamic electron correlation, SCF calculations were performed on the $4f^1$ and $5d^1$ electronic states and were used as reference for second order perturbation calculations where 57 valence electrons were correlated that occupy molecular orbitals with main character Ce 5s, 5p, 4f/5d and Cl 3s, 3p.^{19,20} (The SCF results of the structure and pressure-induced shifts of electronic transitions are in qualitative agreement with those presented here; therefore, the predictions made in this paper already hold qualitatively at that level of theory.) The effects of pressure were modelled by using the AIMP embedding potentials produced in a recent study of high pressure effects on the structure and spectroscopy of V³⁺ defects in $\text{Cs}_2\text{NaYCl}_6$.²¹ The embedding potentials corresponding to a given lattice constant were obtained through self-consistent embedded ions calculations;²¹ they allow to incorporate quantum mechanical interactions with the host $\text{Cs}_2\text{NaYCl}_6$ ions in the $(\text{CeCl}_6)^{3-}$ cluster Hamiltonian.^{15,16} The values of the lattice constant used are listed in Table I, where the corresponding $-\Delta V/V$ values are also shown. These data define a pressure range 1 bar – 26 kbar (see Table I) if the isothermal compressibility of the material is $\kappa = (-\Delta V/V)/\Delta P = 4 \times 10^{-3}$ kbar⁻¹.²¹

Since Ce³⁺ substitute for Y³⁺ ions that occupy O_h sites the embedded cluster energies of all electronic states in the f^1 (the ground state $^2A_{2u}$, $^2T_{2u}$, and $^2T_{1u}$) and d^1 ($^2T_{2g}$ and 2E_g) configurations were calculated at different Ce-Cl distances, R, for each lattice compression (there has been no reports of significant coupling to Jahn-Teller active normal modes). The plots of the potential energy surfaces for ambient pressure and 26 kbar are given in Fig. 1.

We obtained the equilibrium distances, R_e , and totally symmetric vibrational frequencies, $\bar{\nu}_{a_{1g}}$, as in Ref. 21; the vertical (ΔE) and minimum-to-minimum (ΔE_e) transition energies, and the shifts of bond length that occur upon excitation (ΔR_e) were also obtained and are presented in Table I and Figures 1 to 3.

The results in Table I and Fig. 1 show that the Ce–Cl bond length shortens upon $f^1\ ^2A_{2u} \rightarrow d^1\ ^2T_{2g}$ excitation at ambient pressure and at higher pressures as well. Figures 1 and 2 reveal a redshift of the $f^1\ ^2A_{2u} \rightarrow d^1\ ^2T_{2g}$ transition with pressure. Both observations are connected: the sign of the bond length shift determines the sign of the slope of the electronic transition with pressure, being both of them negative, for the $f^1\ ^2A_{2u} \rightarrow d^1\ ^2T_{2g}$ transition. This connection can be established as follows. On the one hand (see Fig 3), the slope of the calculated transition energy ΔE with the Ce–Cl distance R , $d\Delta E/dR$, varies little with pressure (see solid lines) and has the same sign as (and is very similar to) the slope of the minimum-to-minimum transition energy ΔE_e with the Ce–Cl equilibrium distance of the ground state, $d\Delta E_e/dR_e(^2A_{2u})$. The same is true for the slope of the vertical, Frank-Condon transition $\Delta E[R_e(^2A_{2u})]$ with $R_e(^2A_{2u})$, $d\Delta E[R_e(^2A_{2u})]/dR_e(^2A_{2u})$. Furthermore, the observations and conclusions drawn from Fig 3 also apply to any other $i \rightarrow f$ transition studied here, so that

$$\text{sign of } \frac{d\Delta E(i \rightarrow f)}{dR} = \text{sign of } \frac{d\Delta E_e(i \rightarrow f)}{dR_{e,i}}, \quad (1)$$

and their magnitude is similar. On the other hand, it has been shown⁵ that when the force constant of the initial and final states are similar, $k_i \approx k_f \approx k$, like it is the case here (note that $\bar{\nu}_{a_{1g}}$ values are given in Table I and $k = M_{Cl}4\pi^2\bar{\nu}_{a_{1g}}^2c^2$ for the a_{1g} normal mode) the slope of the transition energy $d\Delta E(i \rightarrow f)/dR$ depends basically on the force constant k and on the bond length shift $\Delta R_e(i \rightarrow f) = R_e(f) - R_e(i)$, accompanying the transition, as follows:⁵ $d\Delta E(i \rightarrow f)/dR \approx -k \Delta R_e(i \rightarrow f)$. This, together with the previous observations (Eq. 1), and the fact that $dR_{e,i}/dP \leq 0$, leads to the conclusion that the sign of the slope of a transition with pressure coincides with the sign of the bond length shift that occurs upon excitation:

$$\text{sign of } \frac{d\Delta E_e(i \rightarrow f)}{dP} = \text{sign of } \Delta R_e(i \rightarrow f), \quad (2)$$

and the same is true for the Frank-Condon transition. In effect (Fig 2, Table I), the $f \rightarrow f$ transitions (with $\Delta R_e \approx 0$) are quite insensitive to pressure, $f \rightarrow d(^2T_{2g})$ transitions (with

$\Delta R_e < 0$) shift to the red, and $f \rightarrow d(e_g)$ excitations (with $\Delta R_e > 0$) shift to higher energies with pressure.

It is known, from transition metal spectroscopy, that the so called $10D_q$ transition,²² $d(t_{2g}) \rightarrow d(e_g)$, shifts to high energy values with pressure,^{23,24} which is related to the bond length increase upon $d(t_{2g}) \rightarrow d(e_g)$ excitation (Eq. 2); the same behavior is obtained here for $f^{n-1}d(t_{2g})^1 \rightarrow f^{n-1}d(e_g)^1$ (Table I, Fig 2). It should be noticed, however, that this information alone does not suffice to infer the effects of pressure on the $f \rightarrow d$ transitions; rather, the position of both potential energy surfaces $f^{n-1}d(t_{2g})^1$ and $f^{n-1}d(e_g)^1$ relative to the potential energy surface of the f^n ground state in the R axis of the configurational diagram, has to be also known.⁴ These relative positions have been found to be $R_e[f^{n-1}d(t_{2g})^1] \leq R_e[f^n] \leq R_e[f^{n-1}d(e_g)^1]$ by calculations here and elsewhere, as commented above,⁴ and have been interpreted as resulting from the following simple model of interactions: The inner lanthanide (Ln) (or actinide, An) f^n open-shell electrons are shielded from the ligands by the outer Ln $5p^6$ (An $6p^6$) closed-shell electrons, whose interactions with the ligands determine the bond distance in states of f^n configuration. Instead, upon $f^n \rightarrow f^{n-1}d^1$ excitation one electron has crossed the $5p^6$ ($6p^6$) barrier and becomes exposed to covalent interactions with the ligands, at the same time that it leaves a $4f$ ($5f$) hole behind, available for charge transfer from the ligands, both of which contribute to shortening the bond length between the $f^{n-1}d^1$ baricenter and the ligands. Finally, a large $d(t_{2g})$ - $d(e_g)$ octahedral ligand splitting shortens the $f^{n-1}d(t_{2g})^1$ bond lengths clearly below the f^n ones ($\Delta R_e < 0$) and raises the $f^{n-1}d(e_g)^1$ ones clearly above them ($\Delta R_e > 0$).⁴ These bond length shifts ultimately lead to the predicted red shift of $f^1 \rightarrow d(t_{2g})^1$ and increase of $f^1 \rightarrow d(e_g)^1$ transitions with pressure in $\text{Cs}_2\text{NaYCl}_6:\text{Ce}^{3+}$. Should the sequence of bond lengths be that traditionally assumed: $R_e[f^n] \leq R_e[f^{n-1}d(t_{2g})^1] \leq R_e[f^{n-1}d(e_g)^1]$, both transitions would increase with pressure. Whether the former or the latter sequence of bondlengths actually occurs could be revealed by performing high pressure spectroscopic experiments on this model system $\text{Cs}_2\text{NaYCl}_6:\text{Ce}^{3+}$ in the range 1 bar – 26 kbar.

From all the results we have discussed here it is possible to derive a rule of thumb that can be applied to predict the sign of the change of a transition with pressure. It consists of using the calculated configurational diagram for ambient pressure (dashed lines in Fig 1, for instance) and use it assuming that the effects of pressure simply correspond to moving inwards across the R axis. This approximation applies as a consequence of Eq. (1), which

is a manifestation that the major effect of pressure on these local electronic transitions is a moderate decrease of the f-element – ligand distance.

III. CONCLUSIONS

Previous *ab initio* wavefunction based studies of the structure and spectroscopy of octahedral complexes of *f* element ions in crystals, liquid solutions, and gas phase have shown that the bond length between the *f*-element and the ligands shortens upon $f^n \rightarrow f^{n-1}d(t_{2g})^1$ excitation. This result contradicted the widespread assumption that the bond length is longer in the $f^{n-1}d^1$ states. No experimental proof of the actual sign of the bond length change upon excitation has been given. We have presented here a quantum chemical simulation of spectroscopic experiments under high hydrostatic pressure. The simulation includes scalar relativistic effects, second order perturbation treatment of the valence electron correlation, and quantum mechanical embedding techniques. A continuous redshift of the lowest $f^n \rightarrow f^{n-1}d^1$ band of $\text{Cs}_2\text{NaYCl}_6:\text{Ce}^{3+}$ with pressure is predicted in the range 1 bar to 26 kbar. The pressure-induced redshift is shown to be related to the bond length shortening that accompanies the $f \rightarrow d(t_{2g})$ excitation. Therefore, the simulation points to the experimental detection of the pressure induced redshift as a way to support (or reject) the bond length shortening. More generally, the calculations suggest that the sign of the bond length change upon excitation determines the sign of the pressure-induced shift of the transition, and the effects of pressure on the $f \rightarrow f$ (no shift) and $f \rightarrow d(e_g)$ (shift to higher energies) transitions are also predicted and are related to the respective negligible and positive changes in bond length. The $\text{Cs}_2\text{NaYCl}_6:\text{Ce}^{3+}$ crystal is pointed out as an ideal model system for the counterpart high pressure experimental studies because the higher $f^1 \rightarrow d(e_g)^1$ band has been observed below the cutoff of the host absorption.

ACKNOWLEDGEMENTS

This research was supported in part by Ministerio de Educación y Ciencia, Spain, under contract BQU2002-01316, and Accciones de Movilidad PR2003-0024 and PR2003-0027. We

- ¹ L. Seijo and Z. Barandiarán, *J. Chem. Phys.* **115**, 5554 (2001).
- ² L. Seijo and Z. Barandiarán, *J. Chem. Phys.* **118**, 5335 (2003).
- ³ Z. Barandiarán and L. Seijo, *J. Chem. Phys.* **118**, 7439 (2003).
- ⁴ Z. Barandiarán and L. Seijo, *J. Chem. Phys.* **119**, 3785 (2003).
- ⁵ Z. Barandiarán, N. M. Edelstein, B. Ordejón, F. Ruipérez, and L. Seijo, *J. Solid State Chem.* **178**, 464 (2005).
- ⁶ F. Ruipérez, L. Seijo, and Z. Barandiarán, in preparation.
- ⁷ H. P. Andres, K. Krämer, and H. U. Güdel, *Phys. Rev. B* **54**, 3830 (1996).
- ⁸ Y. Shen and K. L. Bray, *Phys. Rev. B* **58**, 11944 (1998).
- ⁹ N. M. Khaidukov, M. Kirm, S. K. Lam, D. Lo, V. N. Mkhov, and G. Zimmerer, *Opt. Comm.* **184**, 183 (2000).
- ¹⁰ P. J. Dereń, W. Stręk, E. Zych, and J. Drozdzyński, *Chem. Phys. Lett.* **332**, 308 (2000).
- ¹¹ H. G. Drickamer, in *Solid State Physics*, edited by F. Seitz and D. Trunbull (Academic, New York, 1965), Vol. 17, p. 1.
- ¹² K. L. Bray, *Topics in Current Chemistry* (Springer, Berlin, 2001), Vol. 213.
- ¹³ C. S. Yoo, H. B. Radousky, N. C. Holmes and N. M. Edelstein, *Phys. Rev. B* **44**, 830 (1991).
- ¹⁴ P. A. Tanner *et al.*, *J. Amer. Chem. Soc.* **125**, 13225 (2003).
- ¹⁵ Z. Barandiarán and L. Seijo, *J. Chem. Phys.* **89**, 5739 (1988).
- ¹⁶ L. Seijo and Z. Barandiarán, in *Computational Chemistry: Reviews of Current Trends*, edited by J. Leszczyński (World Scientific, Singapore, 1999), Vol. 4, p. 55.
- ¹⁷ L. Seijo, Z. Barandiarán, and B. Ordejón, *Mol. Phys.* **101**, 73 (2003).
- ¹⁸ Z. Barandiarán and L. Seijo, *Can. J. Chem.* **70**, 409 (1992).
- ¹⁹ K. Andersson, P.-Å. Malmqvist, B. O. Roos, A. J. Sadlej, and K. Wolinski, *J. Phys. Chem.* **94**, 5483 (1990).
- ²⁰ K. Andersson, P.-Å. Malmqvist and B. O. Roos, *J. Chem. Phys.* **96**, 1218 (1992).
- ²¹ L. Seijo and Z. Barandiarán, *J. Chem. Phys.* **118**, 1921 (2003).
- ²² S. Sugano, Y. Tanabe, and H. Kamimura, *Multiplets of Transition-Metal Ions in Crystal* (Academic, New York, 1970).

²³ J. F. Dolan, L. A. Kappers, and R. H. Bartram, Phys. Rev. B **33**, 7339 (1986).

²⁴ L. Seijo, Z. Barandiarán, and L. G. M. Pettersson, J. Chem. Phys. **98**, 4041 (1993).

TABLE I: Effects of high pressure on the potential energy surfaces of $4f^1$ and $5d^1$ manifolds of $\text{Cs}_2\text{NaYCl}_6:\text{Ce}^{3+}$. Distances in Å, vibrational frequencies and energies in cm^{-1} .

		lattice constant, a	10.7396	10.6752	10.5463	10.4067	10.3530
		$-\Delta V/V$	0	0.0179	0.0530	0.0902	0.1042
		pressure ^a	1 bar	4.5 kbar	13.2 kbar	22.5 kbar	26 kbar
R_e	$4f^1\ 2A_{2u}$		2.687	2.680	2.664	2.646	2.638
	$2T_{2u}$		2.688	2.681	2.665	2.647	2.639
	$2T_{1u}$		2.690	2.683	2.667	2.649	2.641
	$5d^1\ 2T_{2g}$		2.645	2.639	2.625	2.609	2.602
	$2E_g$		2.705	2.698	2.682	2.662	2.655
	$\langle 5d^1 \rangle^b$		2.669	2.663	2.648	2.630	2.526
ΔR_e	$4f^1\ 2A_{2u} \rightarrow 4f^1\ 2T_{2u}$		0.001	0.001	0.001	0.001	0.001
	$2T_{1u}$		0.003	0.003	0.003	0.003	0.003
	$\rightarrow 5d^1\ 2T_{2g}$		-0.042	-0.041	-0.039	-0.037	-0.036
	$2E_g$		0.018	0.018	0.018	0.016	0.017
	$\rightarrow \langle 5d^1 \rangle$		-0.018	-0.017	-0.016	-0.016	-0.015
	$5d^1\ 2T_{2g} \rightarrow 5d^1\ 2E_g$		0.060	0.059	0.057	0.053	0.053
$\overline{\nu}_{a_{1g}}$	$4f^1\ 2A_{2u}$		306	311	322	335	341
	$2T_{2u}$		306	311	323	336	342
	$2T_{1u}$		307	312	323	336	342
	$5d^1\ 2T_{2g}$		307	312	323	336	341
	$2E_g$		300	305	317	330	336
	ΔE_e		460	460	480	490	500
ΔE_e	$4f^1\ 2A_{2u} \rightarrow 4f^1\ 2T_{2u}$		460	460	480	490	500
	$2T_{1u}$		890	910	950	1000	1020
	$\rightarrow 5d^1\ 2T_{2g}$		24300	24100	23700	23200	23000
	$2E_g$		47200	47300	47700	48100	48200
	$\rightarrow \langle 5d^1 \rangle^c$		33460	33380	33300	33160	33080
	$5d^1\ 2T_{2g} \rightarrow 5d^1\ 2E_g$		22900	23200	24000	24900	25200

^aAssuming $(-\Delta V/V)/P = 4 \times 10^{-3} \text{ kbar}^{-1}$.

^b R_e of $5d^1$ center of gravity = $[3 \times R_e(2T_{2g}) + 2 \times R_e(2E_g)]/5$

^c ΔE_e of $4f^1\ 2A_{2u} \rightarrow 5d^1$ center of gravity = $[3 \times \Delta E_e(2A_{2u} \rightarrow 2T_{2g}) + 2 \times \Delta E_e(2A_{2u} \rightarrow 2E_g)]/5$

FIG. 1: Effects of pressure on the potential energy surfaces of $4f^1$ and $5d^1$ electronic states of $\text{Cs}_2\text{NaYCl}_6:\text{Ce}^{3+}$. High pressure curves (solid lines) correspond to $-\Delta V/V = 0.1042$ (26 kbar, if $\kappa = (-\Delta V/V)/P = 4 \times 10^{-3} \text{ kbar}^{-1}$).

FIG. 2: Effects of pressure on the $4f^1 \rightarrow 4f^1$ and $4f^1 \rightarrow 5d^1$ electronic transitions of $\text{Cs}_2\text{NaYCl}_6:\text{Ce}^{3+}$.

FIG. 3: Solid lines: $4f^1 \ ^2A_{2u} \rightarrow 5d^1 \ ^2T_{2g}$ transition energies versus Ce-Cl distance at different pressures (1 bar and 4.5, 13.2, 22.5, and 26 kbar, respectively, starting from the upper line). Frank-Condon transition energies, $E[^2T_{2g};R_e(^2A_{2u})] - E[^2A_{2u};R_e(^2A_{2u})]$ (circles) and minimum to minimum energies, $E[^2T_{2g};R_e(^2T_{2g})] - E[^2A_{2u};R_e(^2A_{2u})]$ (squares), versus $R_e(^2A_{2u})$ values at different pressures.

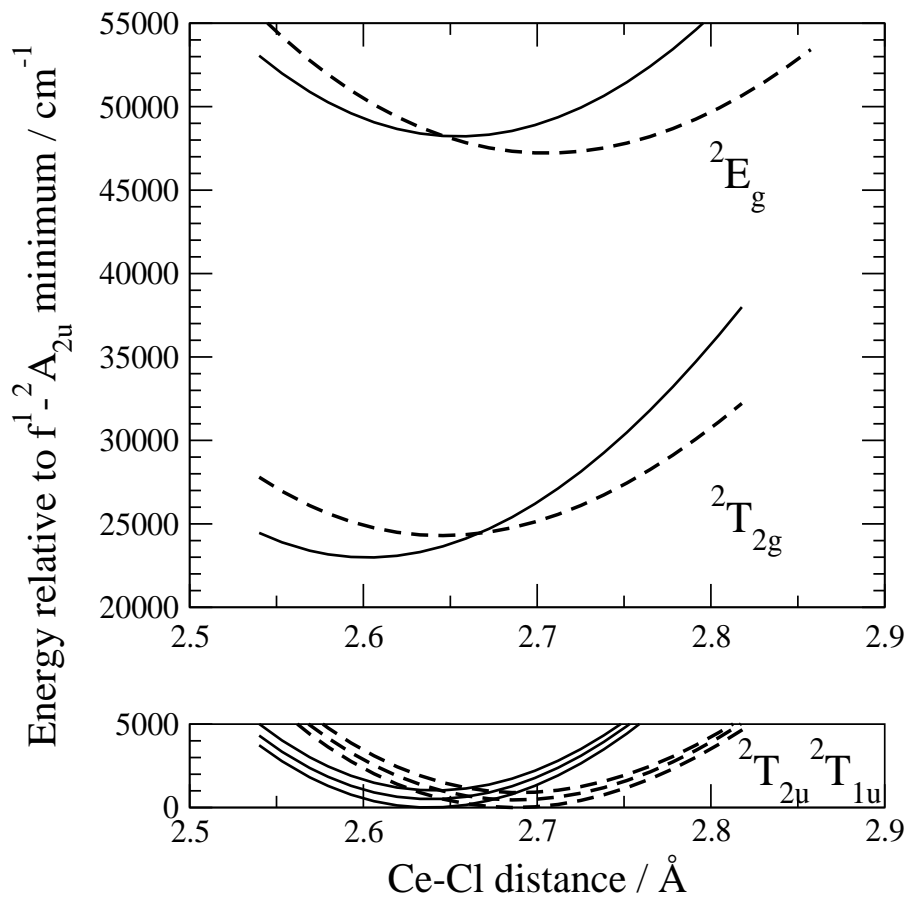


Figure 1. Ruipérez *et al.* Journal of Chemical Physics

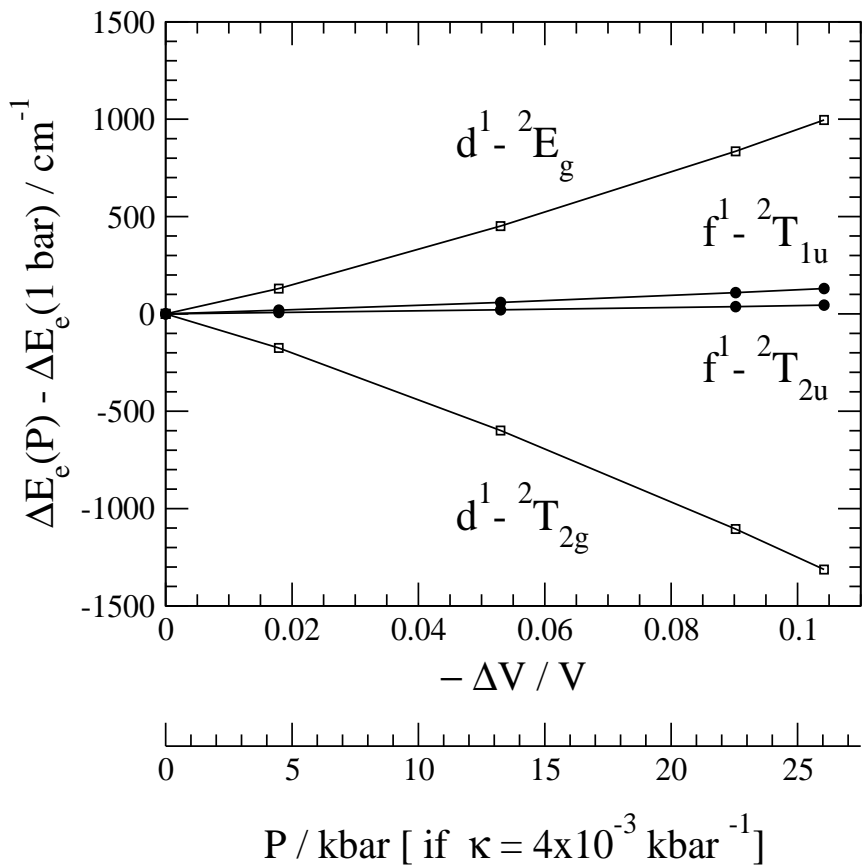


Figure 2. Ruipérez, *et al.* Journal of Chemical Physics

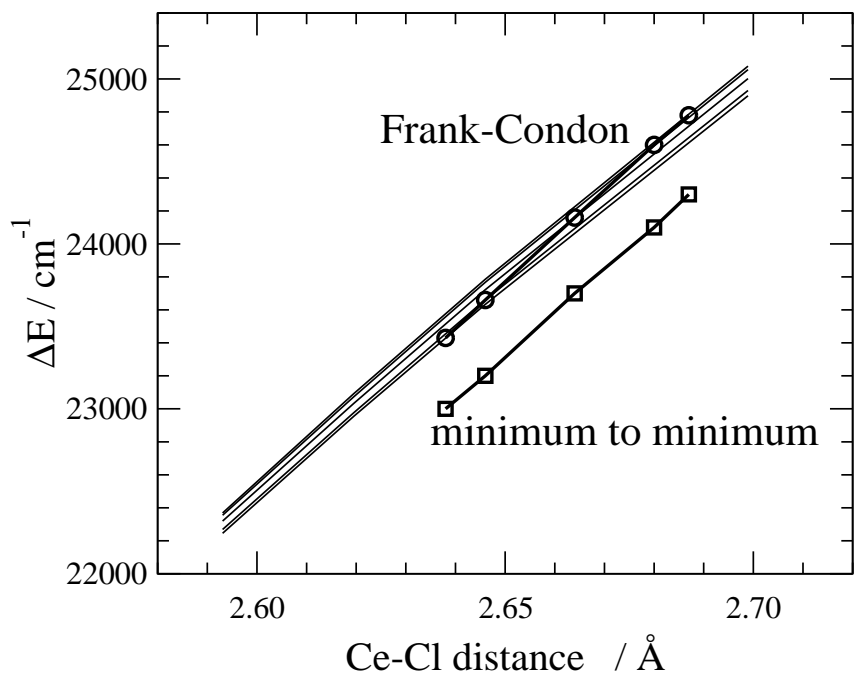


Figure 3. Ruipérez, *et al.* Journal of Chemical Physics